Focal Liver Lesion Classification and Characterization in Noncirrhotic Liver: A Prospective Comparison of Diffusion-Weighted Magnetic

Focal Liver Lesion Classification and Characterization in Noncirrhotic Liver: A Prospective Comparison of Diffusion-Weighted Magnetic Resonance–Related Parameters

Stefano Colagrande, MD Francesco Regini, MD* Filippo Pasquinelli, MD* Lorenzo Nicola Mazzoni, MS† Francesco Mungai, MD* Antonella Filippone, MD‡ and Luigi Grazioli, MD§*

Purpose: The objective of this study was to prospectively verify if diffusion-weighted magnetic resonance (DwMR)–related parameters such as perfusion fraction (f) and slow diffusion coefficient (D), according to Le Bihan theory, are more effective than apparent diffusion coefficient (ADC) for classification and characterization of the more frequent focal liver lesions (FLLs) in noncirrhotic liver.

Methods: Sixty-seven patients underwent standard liver magnetic resonance imaging (MRI) and free-breath multi-b DwMR study. Two regions of interest were defined by 2 observers, including 1 FLL for each patient (21 hemangiomas, 21 focal nodular hyperplasias, 25 metastases) and part of surrounding parenchyma, respectively. For every FLL, D, f, and ADC were estimated both as absolute value and as ratio between FLL and surrounding parenchyma by fitting the reduced equation of the bicompartmental model to experimental data; t test, analysis of variance, and receiver operating characteristic analysis were performed.

Results: t Test showed significant differences in ADC_{lesion}, f_{lesion}, D_{lesion}, ADC_{ratio}, and D_{ratio} values between benign and malignant FLLs, more pronounced for ADC_{lesion} ($P < 0.0009$) and ADC_{ratio} ($P = 0.001$). Applying cutoff values of 1.55×10^{-3} mm^2/s (ADC_{lesion}) and 0.89 (ADC_{ratio}), the DwMR study presented sensitivities and specificities, respectively, of 84% and 80% (for ADC_{lesion}), 72% and 80% (ADC_{ratio}).

Conclusions: Apparent diffusion coefficient (by fitting procedures) better performs than do D and f in FLL classification, especially when its values are less than 1.30 or greater than 2.00×10^{-3} mm^2/s.

Key Words: focal liver lesion, diffusion-weighted imaging, apparent diffusion coefficient (ADC), slow diffusion coefficient (D), perfusion fraction (f), IVIM theory

(*J Comput Assist Tomogr* 2013;37 560–567)

Diffusion-weighted magnetic resonance (DwMR) imaging is an attractive technique that can potentially add useful qualitative and quantitative information to conventional imaging. It is quick (performed within a breath hold or by free breath acquisition) and can be easily incorporated into existing protocols. Finally, it does not require intravenous contrast agent administration; thus, it is easy to repeat and useful in patients with severe renal dysfunction.[1–5]

The use of liver DwMR was initially promising for both detection and classification of focal liver lesions (FLLs),[6] and it is now potentially useful for an early response evaluation after chemotherapy in oncologic patients.[7–13] Although capability in detecting FLLs has been confirmed by various studies,[6,7,14–17] the results regarding the utility of DwMR in FLL classification are contradictory.

Nowadays, it is still unclear whether these challenging conclusions depend on acquisition/postprocessing methods rather than on a physiological low specificity of this technique.[18,19] As far as we know, these results were commonly based on evaluation of apparent diffusion coefficient (ADC) values, which are lower in malignant FLLs than in benign ones, although with wide overlap between the 2 groups.[6,19,20–24]

However, DwMR can provide estimations of other parameters according to the intravoxel incoherent motion (IVIM) theory of Le Bihan et al,[25,26] such as slow diffusion coefficient (D) and perfusion fraction (f). Moreover, in the aforesaid studies, the ADC values were always calculated in the FLLs without any comparison to the surrounding parenchyma.

Given this background, the aim of our prospective study was to compare the performances of ADC, D, and f, both as absolute value and as ratio to surrounding liver parenchyma, for classification/characterization of the more frequent FLLs in patients with no cirrhosis.

MATERIALS AND METHODS

This prospective single-center study, approved by institutional review board (October 18, 2010) was conducted at the University Hospital of (blinded). The study complied with the terms of the Declaration of Helsinki (revision of Edinburgh, 2000).[27] Written consent was obtained from all patients before the examination.

Patients and Study Design

From June 2011 to May 2012, patients with no cirrhosis, who came to our radiology unit for follow-up, with known noncystic FLL(s), were prospectively assessed for eligibility.

The inclusion criterion was the presence of at least 1 hemangioma, focal nodular hyperplasia (FNH) or metastases, measuring no less than 2 cm in maximum diameter and located in the central-lower part of the right liver lobe (where data show higher reproducibility).[18] The exclusion criteria were as follows: underage, history of illegal drug use or alcohol abuse, diffuse liver disease,[28] abnormal liver function tests, and history of liver surgery or interventional liver treatment.

Reference Standard

In this study, the reference standard[29] was the combination of clinical anamnesis and results from previous imaging studies

*From the Department of Experimental and Clinical Biomedical Sciences, Radiodiagnostic Unit, University of Florence, and †Health Physics Section, Azienda Ospedaliero–Universitaria Careggi, Florence; ‡Department of Neurosciences and Imaging, Section of Radiological Imaging, "G. d'Annunzio" University, Chieti; and §Department of Radiology, Spedali Civili, Brescia, Italy.

Received for publication March 1, 2013; accepted March 26, 2013.

Reprints: Stefano Colagrande, MD, Università degli Studi di Firenze, Dipartimento di Scienze Biomediche Sperimentali e Cliniche, Unità Radiodiagnostica n. 2, Azienda Ospedaliero–Universitaria Careggi, Largo Brambilla 3, Firenze, Italy 50134 (e-mail: stefano.colagrande@unifi.it).

This work was partially funded by SIRM (Società Italiana Radiologia Medica).

The authors report no conflicts of interest.

(ultrasonography, magnetic resonance imaging [MRI], computed tomography, biopsy).

All the patients with malignancy received histological confirmation. A full biopsy was performed on the nodule selected for analysis or, if multiple, on a nodule with equivalent imaging pattern. If a patient presented both malignant and benign nodules, only the malignant one was considered, if suitable.

Hemangiomas were defined on computed tomography/MRI typical signal characteristics and contrast enhancement pattern: high and homogeneous signal intensity (SI) on heavily T2-weighted acquisitions (echo time >250 milliseconds) and globular enhancement showing SI similar to that of vessels in every dynamic phase.[30,31]

Focal nodular hyperplasias were diagnosed on unenhanced MRI as being quite isointense to the surrounding parenchyma on T2- and in-phase T1-weighted images, without SI dropout on out-of-phase T1-weighted images. After liver-specific gadolinium chelates contrast agent administration, the diagnostic patterns were hypervascular on arterial phase, without washout on portal and equilibrium phase, and isointense/slight hyperintense to the surrounding parenchyma on biliary phase.[32,33] The central scar is usually seen in nodule larger than 3 cm and appears hypointense and hyperintense with respect to the surrounding parenchyma on unenhanced T1- and T2-weighted images, respectively, with enhancement on portal/equilibrium phase.

Magnetic Resonance Imaging

Magnetic resonance imaging of the liver was performed using a 1.5-T magnetic resonance body scanner (Gyroscan NT Intera Release 12; Philips, Eindhoven, the Netherlands; maximum gradient strength 30 mT/m, peak slew rate 120 mT/m per millisecond) equipped with a 4-channel receiver coil, positioned to cover the upper abdomen of the subject lying in a supine position; the arms were extended over the head to reduce artifacts. All examinations were performed on patients fasting for 6 hours.

Magnetic resonance imaging protocol included the following sequences (Table 1): breath-hold transverse T1-weighted gradient-echo in- and out-of-phase, free-breath transverse and coronal T2-weighted turbo spin-echo, transverse diffusion-weighted free-breath multi-*b*, dynamic 3-dimensional volumetric interpolated breath-hold T1-weighted before and after injection of 0.1 mL per kilogram of GD-EOB-DTPA (gadolinium ethoxybenzyl diethylenetriamine pentaacetic acid, Primovist; Bayer Healthcare, Leverkusen, Germany) also repeated during hepatobiliary phase (at least 20 minutes after the injection).

DwMR Parameters—Diffusion-Related Quantities

DwMR data acquired with different D weightings were processed through the reduced version of the 2 compartments model of IVIM theory,[26]

$$S_b/S_0 = (1-f)\exp(-b \times D) \quad (1)$$

S_b/S_0 is the ratio between the signal obtained with $b \neq 0$ and $b = 0$, f is the perfusion fraction, and D, the slow diffusion coefficient.[25,36–38] f And D were estimated by fitting Eq. 1 to SI data obtained at different b values (from 200 to 800 s/mm^2). This model was adopted considering the absence of data obtained with b values lower than 150 s/mm^2 ($b = 0$ data were excluded): over this threshold, the influence of IVIM from perfusion is reasonably negligible, and monoexponential signal decay is expected. The use of this reduced model implies that fast diffusion coefficient (D*, primarily involved in SI variations between $b = 0$ and 200 s/mm^2) was not calculated.[25,26,33–36] Apparent diffusion coefficient was estimated with a similar procedure, fitting the following equation to SI data obtained at different b values (from 0 to 800 s/mm^2):

$$S_b/S_0 = \exp(-b \times \mathrm{ADC}) \quad (2)$$

The main difference between the first and the second fitting procedure is that $b = 0$ data are used only for ADC estimation (Eq. 1). All calculations were performed using semiautomatic homemade software driving the nonlinear regression algorithms provided in Gnuplot (http://www.gnuplot.info/, 4.4.2 release).

Sampling Method and Diffusion-Weighted Images Analysis

The sampling of FLL was performed with freehand-drawn region of interest (ROI) inscribing the entire lesion and avoiding lesion boundary, necrotic areas, and vessels. Region of interest was defined on $b = 0$ images and then copied over all other D-weighted images using ImageJ.[38] In case of multiple FLLs in the medium-lower part of the right lobe, the one showing the highest diffusion-weighted signal homogeneity at visual

TABLE 1. Sequence Details

Sequence	TR/TE, ms/Flip Angle, degrees	NSA	Matrix	FOV, mm	Slice Thickness, mm/n	Bandwidth, Hz/pixel	TA, s
T1-weighted 2-dimensional gradient echo in-/out-of-phase	184/4.6–2.3/80	1	192 × 110	280–400	6/24	1002	17
T2-weighted single-shot turbo spin-echo (SSH)	∞/80/90	1	268 × 150	290–415	4/48	518	120/180
T1-weighted 3-dimensional gradient echo (THRIVE)*	3.5/1.6/10	1	164 × 114	285–400	1.5/80	530	18
DwI SSH EPI†	2000/66/90	2	128 × 65	300–420	7/12	1555	140

All sequences were acquired with parallel imaging SENSE factor 1.5, but diffusion-weighted images were obtained without SENSE factor due to software limitation (Philips Intera, release 12.1).

*THRIVE (T1-weighted high-resolution isotropic volume examination) sequences were performed before and repeated 3 times at 30-, 70-, 180-second intervals after contrast agent and at 20 minutes during hepatobiliary phase.

†Five b values: 0, 200, 400, 600, and 800 s/mm^2.

TR, repetition time; TE, echo time; NSA, number of signal averages; TA, acquisition time; FOV, field of view; DwI, diffusion-weighted imaging; EPI, echo-planar imaging.

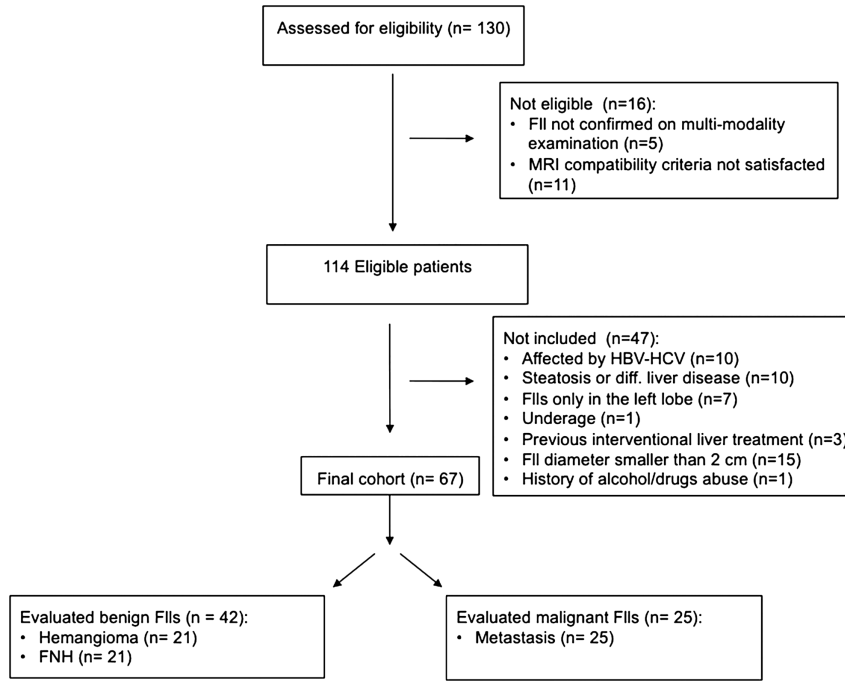

FIGURE 1. Flowchart for patient selection.

assessment and the lowest SD measured at different b values was chosen.

For every FLL, an ROI of similar size was drawn in the adjacent healthy liver parenchyma, excluding large blood vessels, biliary vessels, and hepatic borders, to calculate diffusion-weighted–related parameters not only as absolute values (f_{lesion}, D_{lesion}, $\text{ADC}_{\text{lesion}}$) but also as ratios to normal parenchyma ($\frac{f_{\text{lesion}}}{f_{\text{parenchyma}}}$,$\frac{D_{\text{lesion}}}{D_{\text{parenchyma}}}$, and $\frac{\text{ADC}_{\text{lesion}}}{\text{ADC}_{\text{parenchyma}}}$) reported in the following as f_{ratio}, D_{ratio}, and $\text{ADC}_{\text{ratio}}$, respectively). This was done to obtain more reproducible results and decrease the dependence from b value. Every lesion and surrounding parenchyma received 3 measurements, and values were averaged. Diffusion-weighted images and ROI shapes were evaluated in consensus by a radiologist and a physicist (F.R and L.N.M.) and then finally checked by the study coordinator (S.C.). When they expressed discordant opinions about a value of one of the estimated parameters (>5% difference), they reached a consensus through a joint review.

We checked the stability of our scanner by doing an DwMR phantom study,[18] as recommended.[34] The phantom was scanned 10 times during the period of the study, applying a diffusion-weighted sequence $b = 0 - 1000$ s/mm^2 (with steps of 100 s/mm^2). Apparent diffusion coefficient was calculated by fitting Eq. 2 to the acquired data. The ADC variation with respect to baseline was estimated.

Statistical Analysis

Levene test was performed on each of the 6 variables (f_{lesion}, D_{lesion}, $\text{ADC}_{\text{lesion}}$, f_{ratio}, D_{ratio}, $\text{ADC}_{\text{ratio}}$), to evaluate the homogeneity of variance among the various histotypes (hemangioma, FNH, metastasis). Analysis of variance (ANOVA) was performed on the same variables, to evaluate differences among the mean values of the 3 different groups. In case of significant differences, detected by ANOVA, Games-Howell and Bonferroni post hoc tests were applied, respectively, in case of significant or nonsignificant differences among groups variance, revealed by Levene test (significance threshold was set at $P < 0.05$). Descriptive statistic was also calculated for each group.

t Test for independent groups was performed to establish differences between benign and malignant lesions, assuming or not the agreement of variance depending on Levene test results. Afterward, a receiver operating characteristic (ROC) analysis was performed, calculating the areas under the curve for each variable. All the latter values were subsequently compared, to identify the set of DwMR parameters most useful in differentiating and identifying benign and malignant FLLs, excluding from further analysis those parameters showing significant differences from the best one (statistical significance was set at $P < 0.05$).

Finally, sensitivity and specificity for malignancy were calculated on the whole spectrum of values of the selected best variables. Sensitivity represents the percentage of malignant lesions that the test variable identifies as malignant, whereas specificity represents the percentage of benign lesions that the test variable identifies as benign. Statistical analysis was performed using STATA 10.2 (Stata Corp, College Station, Tex).

RESULTS

One-hundred thirty consecutive patients were assessed for eligibility. Sixteen patients were excluded because of not satisfying the magnetic resonance compatibility criteria or because the presence of a solid FLL could not be confirmed with standard MRI. Subsequently, 47 patients were excluded because of not satisfying the inclusion criteria and because of standard MRI findings.

Therefore, the final cohort included 67 patients (43 men, 24 women; mean age, 58.5 years; age range, 27–81 years). There were 25 patients with history of primary malignancy: colon cancer (n = 10), breast cancer (n = 8), gastric cancer (n = 4), and pancreatic cancer (n = 3). We finally studied 42 benign

TABLE 2. Mean ± SD and CV of Diffusion-Weighted Imaging–Related Parameters for Each Group of FLLs

Parameters	HE	FNH	MTX
f_{lesion}	20 ± 12 (60)	22 ± 13 (59)	13 ± 7 (54)
D_{lesion}	1.53 ± 0.54 (35)	1.25 ± 0.39 (32)	1.05 ± 0.41 (39)
ADC_{lesion}	2.24 ± 0.96 (43)	1.86 ± 0.42 (23)	1.31 ± 0.47 (36)
f_{ratio}	0.66 ± 0.27 (41)	0.65 ± 0.25 (38)	0.44 ± 0.16 (36)
D_{ratio}	1.45 ± 0.46 (32)	1.13 ± 0.39 (35)	1.02 ± 0.44 (43)
ADC_{ratio}	1.21 ± 0.46 (38)	1.05 ± 0.23 (22)	0.79 ± 0.26 (33)

Mean ± SD and coefficient of variation (CV, %) in brackets of perfusion fraction (f, %), diffusion coefficient (D, in $\times 10^{-3}$ mm^2/s), ADC of the lesion (in $\times 10^{-3}$ mm^2/s), and corresponding ratios with healthy liver parenchyma measurements.

HE, hemangioma; MTX, metastasis.

(21 hemangiomas and 21 FNHs) and 25 malignant FLLs (metastases) (Fig. 1), all of them situated in the medium-lower part of the right lobe. Mean diameter of lesions was 2.7 cm (range, 2–4.8 cm).

Our scanner showed good stability, comparable with what has already been reported[18]: repeatability- and reproducibility-related errors were always less than 0.8%.[37]

Subgroups: Characterization

Levene test established significant differences among groups for f_{lesion}, ADC_{lesion}, and ADC_{ratio} variances so Bonferroni or Games-Howell post hoc tests were consequently adopted. For each group, mean and SD of f_{lesion}, D_{lesion}, ADC_{lesion}, f_{ratio}, D_{ratio}, and ADC_{ratio} are reported (Tables 2 and 3, Fig. 2). Analysis of variance showed significant differences of D_{lesion}, ADC_{lesion}, D_{ratio}, and ADC_{ratio} among different groups (Table 4).

Benign Versus Malignant: Classification

Levene test established significant differences among groups for the variance of f_{lesion}: for this variable, the hypothesis of different variances was adopted in the t test.

For each group, mean and SD of f_{lesion}, D_{lesion}, ADC_{lesion}, f_{ratio}, D_{ratio}, and ADC_{ratio} are reported. t Test showed significant differences of f_{lesion}, D_{lesion}, ADC_{lesion}, D_{ratio}, and ADC_{ratio} among benign and malignant FLLs groups: corresponding P values are reported (Table 2). The area under the curve of the ROC analysis was maximum for ADC_{lesion}, and only ADC_{ratio} showed nonsignificant difference with the former ($P = 0.11$, Fig. 3): all other variables were excluded from further analysis. Cumulative frequencies for these variables are reported (Fig. 4).

Sensitivity (with 95% confidence interval) corresponding to a specificity of 80% was 84% (50%–97%) for $ADC_{lesion} = 1.55 \times 10^{-3}$ mm^2/s and 72% (40%–92%) for $ADC_{ratio} = 0.89$. Finally, percentage distribution of benign and malignant FLLs for various intervals of ADC_{lesion} values was calculated.

DISCUSSION

Our data brought good results in terms of statistically significant differences between malignant and benign FLLs for most of the parameters evaluated, either as absolute values or as ratio, even if showing overlap between the 2 groups.

Many articles[14,18,24] have shown the large variability of the ADC in FLLs, which strongly depends on the b values adopted.[18] There are other parameters according IVIM theory, which are less dependent on the choice of the b value acquisition, such as D and f. However, calculation of these parameters is time-consuming in either acquisition (for a multi-b free-breath sequence, at least 4 minutes is needed) or postprocessing (manual evaluation). Then we wondered if this additional time and work would have been useful and if non–ADC-related parameters would better perform than ADC itself in FLL classification characterization. To the best of our knowledge, this is the first attempt to carry out this comparison even if other studies evaluated non–ADC-related parameters in normal and pathologic liver.[39–41]

The physiological interpretation, proposed for the first time by Le Bihan et al,[25,26,42] is that D represents the slow diffusion coefficient, related to thermal diffusion of water molecules, whereas f is the fraction of water molecules flowing inside the capillary network. Both can be better estimated using a series of diffusion-weighted images with $b \geq 200$ s/mm^2. Le Bihan et al[25,26,37,43] proposed another parameter used to represent the influence of nondiffusional IVIM on DwMR signal: the coefficient D^*, related to the random flow within capillary network (fast motion). We did not evaluate it because it was affected by a strong experimental error[25,26,37,43] mainly

TABLE 3. Mean ± SD and CV of Diffusion-Weighted Imaging–Related Parameters for Benign and Malignant FLLs

Parameters	Benign Lesions (B = HE + FNH)	Malignant Lesions (M = MTX)	P, B vs M
f_{lesion}	20 ± 8 (40)	13 ± 7 (54)	0.03
D_{lesion}	1.39 ± 0.49 (35)	1.05 ± 0.41 (39)	0.004
ADC_{lesion}	2.05 ± 0.76 (37)	1.31 ± 0.47 (36)	<0.0009
f_{ratio}	0.65 ± 0.22 (34)	0.44 ± 0.16 (36)	0.33
D_{ratio}	1.30 ± 0.45 (35)	1.02 ± 0.44 (43)	0.02
ADC_{ratio}	1.13 ± 0.43 (38)	0.79 ± 0.26 (33)	0.001

Mean ± SD and coefficient of variation (CV, %) in brackets of perfusion fraction (f, %), diffusion coefficient (D, in $\times 10^{-3}$ mm^2/s), ADC of the lesion (in $\times 10^{-3}$ mm^2/s), and corresponding ratios with healthy liver parenchyma measurements. P value is given for benign versus malignant lesions.

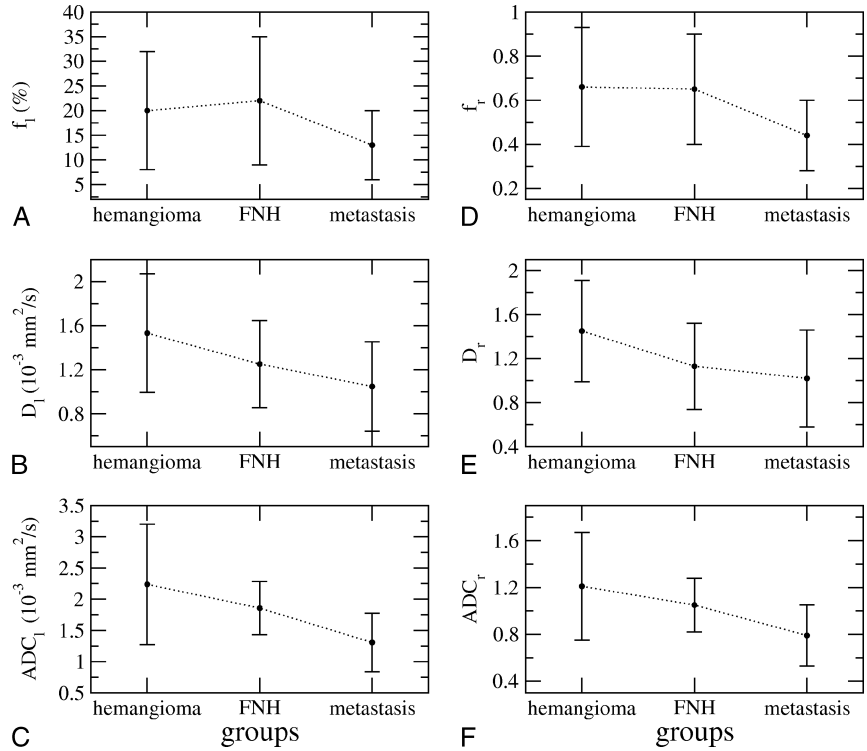

FIGURE 2. Mean values and SD of every parameter evaluated (f_{lesion}, D_{lesion}, ADC_{lesion}, f_{ratio}, D_{ratio}, ADC_{ratio}) for each group of lesions (hemangioma, FNH, metastasis). Levene test shows significant differences between hemangioma and metastasis for ADC_{lesion}, D_{lesion}, ADC_{ratio}, and D_{ratio} and between FNH and metastasis for ADC_{lesion}. l Indicates lesion; r, ratio.

due to low b value acquisition and because adopting high b values allows more accurate ADC estimation.

In our study, ADC performs better than do f and D. All these parameters, in fact, show a significant difference between benign and malignant lesions and between hemangiomas and metastases, but only ADC values show significant differences between FNHs and metastases. Within the group of benign FLLs, there is no significant quantitative difference between FNH and hemangioma. Malignant lesions show lower ADC, f, and D values than benign lesion (Table 2). This could be due to the presence of more restricted diffusion and lower perfusion within the metastatic lesions.[44] The best performances (higher sensitivity and specificity) obtained with ADC parameter compared with D and f probably relate to ADC features, being expression of both perfusion- and diffusion-related motions.

Although there are quite good results in terms of significant differences between malignant and benign FLLs, clinical applications of DwMR-related parameters in FLL classification are in our opinion still limited, but not unhelpful at all. Quantitative analysis could be used as added criterion together with a qualitative DwMR analysis[45] and other traditional sequences[46]; this might be especially useful when contrast agent cannot be administered. Moreover, even if our results show overlap between benign and malignant lesions, especially for ADC values between 1.30 and 2.00 $\times$ 10^{-3} mm^2/s (with 57% of benign lesions and 35% of malignant ones within this range), ADC values less than 1.30 $\times$ 10^{-3} mm^2/s are most likely present in metastases (only 5% of benign FLLs are below this threshold), whereas ADC values greater than 2.00 $\times$ 10^{-3} mm^2/s are reasonably a sign of benignity (only 5% of metastases are over this threshold) (Figs. 2–4). In our study, ADC is not calculated on ADC maps obtained using SI ratio from only 2 images, with and without D weighting (ie, $b = 0$ and $b \neq 0$, respectively), as usually performed automatically by commercial magnetic resonance scanner. In a phantom showing monoexponential signal decay, results obtained using these 2 methods are not

TABLE 4. ANOVA Results

	Parameter					
	f_{lesion}	D_{lesion}	ADC_{lesion}	f_{ratio}	D_{ratio}	ADC_{ratio}
Significant for	NS	Hemangioma vs metastasis ($P = 0.002$)	Hemangioma vs metastasis ($P < 0.0009$), FNH vs metastasis ($P = 0.001$)	NS	Hemangioma vs metastasis ($P = 0.006$)	Hemangioma vs metastasis ($P = 0.001$)

Significant differences of all the diffusion-weighted imaging parameters estimated in the lesion and as ratios with healthy liver parenchyma among different group of lesions and corresponding P values.

NS indicates not statistically significant.

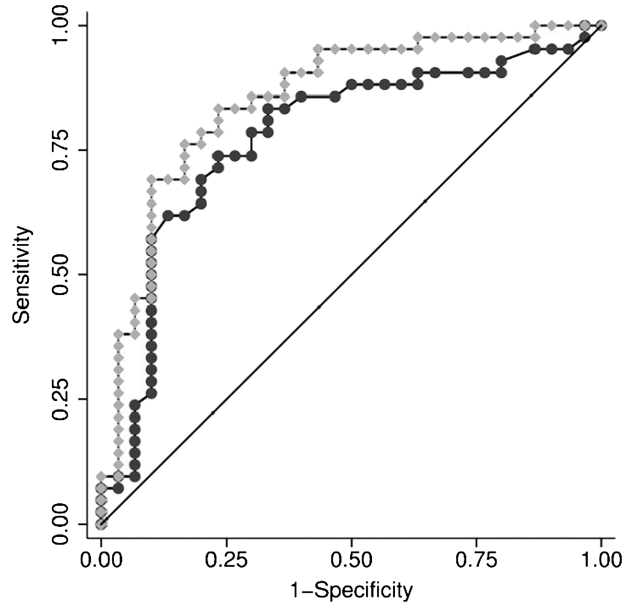

FIGURE 3. ROC analysis. The area under the curve (AUC) of the ROC analysis was maximum for ADC_{lesion} (gray diamonds), and only ADC_{ratio} (black circles) AUC showed nonsignificant difference with the former ($P = 0.11$).

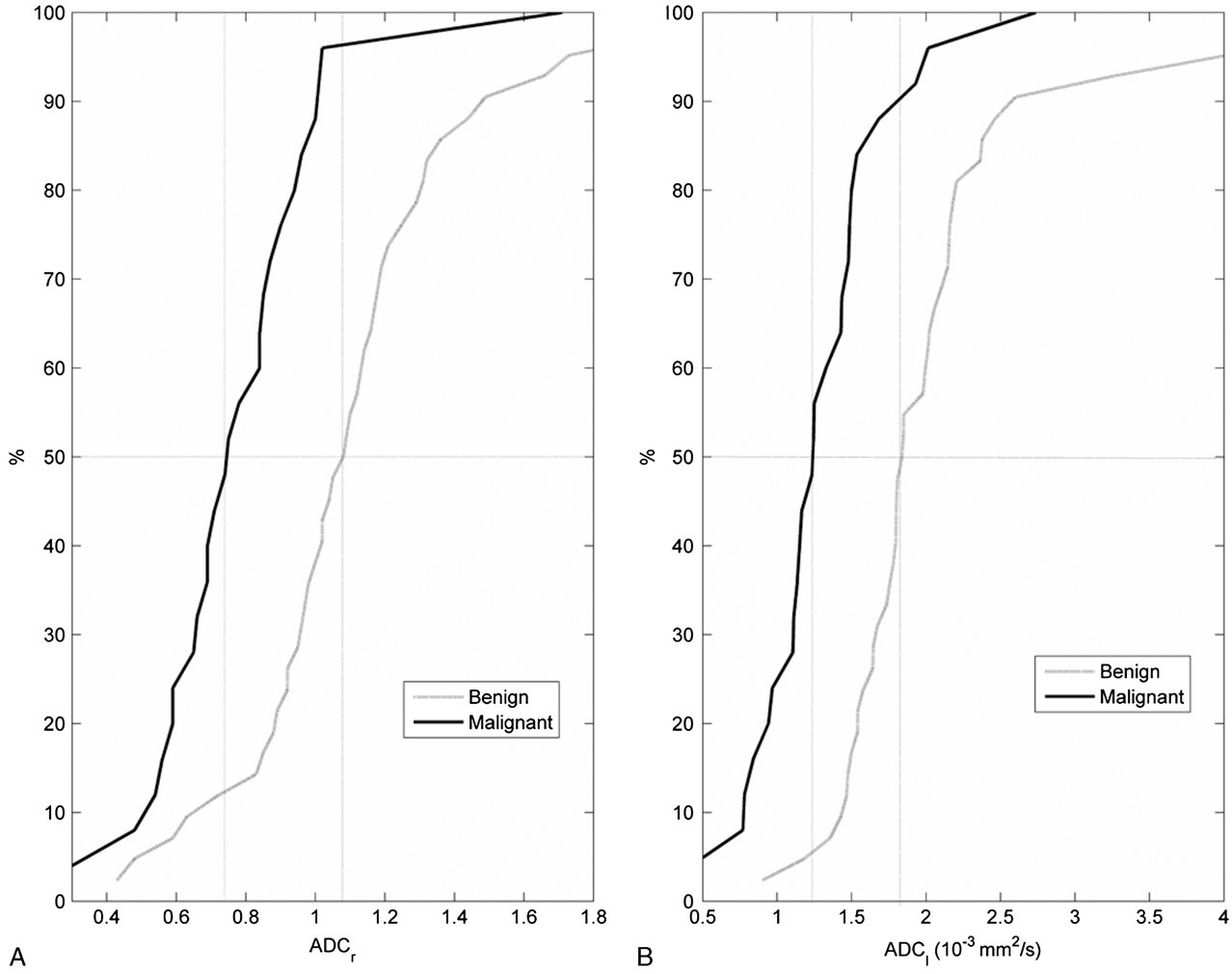

FIGURE 4. Cumulative frequencies of ADCr (A) and ADCl (B) both for benign and malignant focal liver lesions.

different[18]; this is not true in the liver parenchyma, where a biexponential signal decay is expected.[25] In this case, the use of the mentioned best-fitting procedure was performed in ADC too, to achieve results comparable with *f* and *D*. Calculation brings results that are less dependent on SI at every *b* value and should be then more accurate and reproducible,[47] even if time consuming.

The use of parameters as ratio brought no relevant contribution to the value of DwMR in FLL characterization because of the increased measurement error, as expected. However, in our opinion, ratio could have some utility, further decreasing the *b* dependency and allowing to better compare DwMR acquisition performed with different *b* values. On this background, although in the ratio evaluation the reference organ is usually the spleen,[48,49] in our assessment we preferred the adoption of the adjacent hepatic parenchyma, to have the advantage of using the same level of slice for ROI placement and consequently the equivalent field heterogeneity. In fact, in our experience, with a ratio greater than 1 or less than 0.8 the probability to respectively have benignity or malignancy is around 90% (Fig. 4). So, the evaluation is fast, simple, and reproducible, and this could be useful in the everyday practice.

The main weakness of the study could be represented by the few histotypes included using very selective enrollment criteria. However, we chose this study design because we did not need many different histotypes to achieve the proposed comparison among parameters. This study was planned to find out what diffusion-weighted–related parameter and quantitative method were the best (the more reproducible and the less affected by artifacts on a scanner without navigator echo). Our strategy was to perform the assessment in the best conditions; thus, we had cared to avoid lesions too small to be sampled, as well as those localized in the left lobe and/or at the top/bottom of the liver, where artifacts are usually present. Moreover, it would have been very difficult to enroll a group of primary malignancies (hepatocellular carcinoma and cholangiocellular carcinoma) and of adenomas with a similar number of cases of the selected groups. Finally, mean ADC value of adenoma is usually not dissimilar from that of FNH,[45] whereas values of hepatocellular carcinoma and cholangiocellular carcinoma are comparable to those of metastases.[50]

The great overlap between benign and malignant nodules found in our and other series[50] drives us to argue that in almost half of the cases DwMR does not have the sensitivity to detect the obvious difference in architecture, cellularity, and perfusion among hemangioma, FNH, and metastases, even adopting IVIM theory and non–ADC DwMR-related parameters. Then, according to our series, ADC (absolute value and ratio) allows for the best quantitative analysis. Further investigations should be done to estimate differences in performance between fitted ADC (non–*b*-related and time consuming) and nonfitted ADC (*b*-related and not time consuming).

In conclusion, our results, by fitting procedure, show that ADC as absolute value better performs than do *D* and *f* in FLL classification and can be supportive in the diagnosis as supplemental criterion of benignity or malignancy.

REFERENCES

1. Taouli B, Koh DM. Diffusion-weighted MR imaging of the liver. *Radiology.* 2010;254:47–66.
2. Grobner T. Gadolinium—a specific trigger for the development of nephrogenic fibrosing dermopathy and nephrogenic systemic fibrosis? *Nephrol Dial Transplant*. 2006;21:1104–1108.
3. Sadowski EA, Bennett LK, Chan MR, et al. Nephrogenic systemic fibrosis: risk factors and incidence estimation. *Radiology.* 2007; 243:148–157.
4. Marckmann J, Skav L, Rossen K, et al. Nephrogenic systemic fibrosis: suspected causative role of gadodiamide used for contrast-enhanced magnetic resonance imaging. *Am Soc Nephrol*. 2006;17:2359–2362.
5. Thomsen HS, Marckmann P, Logager VB. Update on nephrogenic systemic fibrosis. *Magn Reson Imaging Clin N Am*. 2008;16:551–560.
6. Parikh T, Drew SJ, Lee VS, et al. Focal liver lesion detection and characterization with diffusion-weighted MR imaging: comparison with standard breath-hold T2-weighted imaging. *Radiology.* 2008; 246:812–822.
7. Bonekamp S, Corona-Villalobos CP, Kamel IR. Oncologic applications of diffusion-weighted MRI in the body. *J Magn Reson Imaging*. 2012; 35:257–279.
8. Marugami N, Tanaka T, Kitano S, et al. Early detection of therapeutic response to hepatic arterial infusion chemotherapy of liver metastases from colorectal cancer using diffusion-weighted MR imaging. *Cardiovasc Intervent Radiol*. 2009;32:638–646.
9. Charles-Edwards EM, De Souza NM. Diffusion-weighted magnetic resonance imaging and its application to cancer. *Cancer Imaging*. 2006;6:135–143.
10. De Keyzer F, Vandecaveye V, Thoeny H, et al. Dynamic contrast-enhanced and diffusion-weighted MRI for early detection of tumoral changes in single-dose and fractionated radiotherapy: evaluation in a rat rhabdomyosarcoma model. *Eur Radiol*. 2009;19:2663–2671.
11. Koh DM, Takahara T, Imai Y, et al. DJ. Practical aspects of assessing tumors using clinical diffusion-weighted imaging in the body. *Magn Reson Med Sci*. 2007;6:211–224.
12. Kwee TC, Takahara T, Ochiai R, et al. Whole-body diffusion-weighted magnetic resonance imaging. *Eur J Radiol*. 2009;70:409–417.
13. Lee CH, Braga L, de Campos RO, et al. Hepatic tumor response evaluation by MRI. *NMR Biomed*. 2011;24:721–733.
14. Holzapfel K, Eiber MJ, Fingerle AA, et al. Detection, classification, and characterization of focal liver lesions: value of diffusion-weighted MR imaging, gadoxetic acid–enhanced MR imaging and the combination of both methods. *Abdom Imaging*. 2012;37:74–82.
15. Chandarana H, Taouli B. Diffusion-weighted MRI and liver metastases. *Magn Reson Imaging Clin N Am*. 2010;18:451–464.
16. Eiber M, Fingerle AA, Brügel M, et al. Detection and classification of focal liver lesions in patients with colorectal cancer: retrospective comparison of diffusion-weighted MR imaging and multi-slice CT. *Eur J Radiol*. 2011;81:683–691.
17. Koh DM, Brown G, Riddell AM, et al. Detection of colorectal hepatic metastases using MnDPDP MR imaging and diffusion-weighted imaging (DWI) alone and in combination. *Eur Radiol*. 2008;18:903–910.
18. Colagrande S, Pasquinelli F, Mazzoni LN, et al. MR-diffusion weighted imaging of healthy liver parenchyma: repeatability and reproducibility of apparent diffusion coefficient measurement. *J Magn Reson Imaging*. 2010;31:912–920.
19. Holzapfel K, Brügel M, Eiber M, et al. Characterization of small (=10 mm) focal liver lesions: value of respiratory-triggered echo-planar diffusion-weighted MR imaging. *Eur J Radiol*. 2010;76:89–95.
20. Miller FH, Hammond N, Siddiqi AJ, et al. Utility of diffusion-weighted MRI in distinguishing benign and malignant hepatic lesions. *J Magn Reson Imaging*. 2010;32:138–147.
21. Chandarana H, Taouli B. Diffusion and perfusion imaging of the liver. *Eur J Radiol*. 2010;76:348–358.
22. Soyer P, Corno L, Boudiaf M, et al. Differentiation between cavernous hemangiomas and untreated malignant neoplasms of the liver with free-breathing diffusion-weighted MR imaging: comparison with T2-weighted fast spin-echo MR imaging. *Eur J Radiol*. 2011;80:316–324.

23. Gourtsoyianni S, Papanikolaou N, Yarmenitis S, et al. Respiratory gated diffusion-weighted imaging of the liver: value of apparent diffusion coefficient measurements in the differentiation between most commonly encountered benign and malignant focal liver lesions. *Eur Radiol*. 2008;18:486–492.
24. Sandrasegaran K, Akisik FM, Lin C, et al. The value of diffusion-weighted imaging in characterizing focal liver masses. *Acad Radiol*. 2009;16:1208–1214.
25. Le Bihan D, Breton E, Lallemand D, et al. Separation of diffusion and perfusion in intravoxel incoherent motion MR imaging. *Radiology.* 1988;168:497–505.
26. Le Bihan D. Intravoxel incoherent motion perfusion MR imaging: a wake-up call. *Radiology.* 2008;249:891–899.
27. World Medical Association Declaration of Helsinki: ethical principles for medical research involving human subjects. *JAMA*. 2000;284: 3043–3045.
28. Outwater EK, Blasbalg R, Siegelman ES, et al. Detection of lipid in abdominal tissues with opposed-phase gradient-echo images at 1.5 T: techniques and diagnostic importance. *Radiographics*. 1998;18:1465–1480.
29. Bossuyt PM, Reitsma JB, Bruns DE, et al. Standards for reporting of diagnostic accuracy. Towards complete and accurate reporting of studies of diagnostic accuracy: the STARD Initiative. *Radiology.* 2003;226:24–28.
30. Whitney WS, Herfkens RJ, Jeffrey RB, et al. Dynamic breath-hold multiplanar spoiled gradient-recalled MR imaging with gadolinium enhancement for differentiating hepatic hemangiomas from malignancies at 1.5 T. *Radiology.* 1993;189:863–870.
31. Semelka RC, Brown ED, Ascher SM, et al. Hepatic hemangiomas: a multi-institutional study of appearance on T2-weighted and serial gadolinium-enhanced gradient-echo MR images. *Radiology.* 1994;192:401–406.
32. Grazioli L, Morana G, Kirchin MA, et al. Accurate differentiation of focal nodular hyperplasia from hepatic adenoma at gadobenate dimeglumine–enhanced MR imaging: prospective study. *Radiology.* 2005;236:166–177.
33. Grazioli L, Bondioni MP, Haradome H, et al. Hepatocellular adenoma and focal nodular hyperplasia: value of gadoxetic acid–enhanced MR imaging in differential diagnosis. *Radiology.* 2012;262:520–529.
34. Padhani AR, Liu G, Koh DM, et al. Diffusion-weighted magnetic resonance imaging as a cancer biomarker: consensus and recommendations. *Neoplasia*. 2009;11:102–125.
35. Luciani A, Vignaud A, Cavet M, et al. Liver cirrhosis: intravoxel incoherent motion MR imaging-pilot study. *Radiology.* 2008;249:891–899.
36. Patel J, Sigmund EE, Rusinek H, et al. Diagnosis of cirrhosis with intravoxel incoherent motion diffusion MRI and dynamic contrast-enhanced MRI alone and in combination: preliminary experience. *J Magn Reson Imaging*. 2010;31:589–600.
37. Pasquinelli F, Belli G, Mazzoni LN, et al. Magnetic resonance diffusion-weighted imaging: quantitative evaluation of age-related changes in healthy liver parenchyma. *Magn Reson Imaging*. 2011;29:805–812.
38. Abramoff MD, Magalhaes PJ, Ram SJ. Image processing with Image J. *Biophotonics International 1*. 2011;1:36–42.
39. Dijkstra H, Baron P, Kappert P, et al. Effects of microperfusion in hepatic diffusion weighted imaging. *Eur Radiol*. 2012;22:891–899.
40. Yamada L, Aung W, Himeno Y, et al. Diffusion coefficients in abdominal organs and hepatic lesions: evaluation with intravoxel incoherent motion echo-planar MR imaging. *Radiology.* 1999;210: 617–623.
41. Coenegrachts K, Delanote J, Ter Beek L, et al. Evaluation of true diffusion, perfusion factor, and apparent diffusion coefficient in non-necrotic liver metastases and uncomplicated liver hemangiomas using black-blood echo planar imaging. *Eur J Radiol*. 2009;69:131–138
42. Le Bihan D, Breton E, Lallemand D, et al. MR imaging of intravoxel incoherent motions: application to diffusion and perfusion in neurologic disorders. *Radiology.* 1986;161:401–407.
43. Pasquinelli F, Belli G, Mazzoni LN, et al. MR-diffusion imaging in assessing chronic liver diseases: does a clinical role exist? *Radiol Med*. 2012;117:242–253.
44. Edrei Y, Gross E, Corchia N, et al. Vascular profile characterization of liver tumors by magnetic resonance imaging using hemodynamic response imaging in mice. *Neoplasia*. 2011;13:244–253.
45. Agnello F, Ronot M, Valla DC, et al. High-b-Value Diffusion-weighted MR Imaging of benign hepatocellular lesions: quantitative and qualitative analysis. *Radiology.* 2012;262:511–519.
46. Haradome H, Grazioli L, Morone M, et al. T2-weighted and diffusion-weighted MRI for discriminating benign from malignant focal liver lesions: diagnostic abilities of single versus combined interpretations. *J Magn Reson Imaging*. 2012;35:1388–1396.
47. Chandarana H, Lee VS, Hecht E, et al. Comparison of biexponential and monoexponential model of diffusion weighted imaging in evaluation of renal lesions: preliminary experience. *Invest Radiol*. 2011;46:285–291.
48. Papanikolaou N, Gourtsoyianni S, Yarmenitis S, et al. Comparison between two-point and four-point methods for quantification of apparent diffusion coefficient of normal liver parenchyma and focal lesions. Value of normalization with spleen. *Eur J Radiol*. 2010;73:305–309.
49. Do RK, Chandarana H, Felker E, et al. Diagnosis of liver fibrosis and cirrhosis with diffusion-weighted imaging: value of normalized apparent diffusion coefficient using the spleen as reference organ. *AJR Am J Roentgenol*. 2010;195:671–676.
50. Xia D, Jing J, Shen H, et al. Value of diffusion-weighted magnetic resonance images for discrimination of focal benign and malignant hepatic lesions: a meta-analysis. *J Magn Reson Imaging*. 2010;32:130–137.